Armed Services Technical Information Agency

AD 37716

Columbia University
in the City of New York

DEPARTMENT OF CIVIL ENGINEERING
AND ENGINEERING MECHANICS

RESIDUAL STRESS IN GLASS SPHERES

by

L. RONGVED

RESIDUAL STRESS IN GLASS SPHERES

ABSTRACT

The problem of thermal stress in a Maxwell body is formulated mathematically for the case of symmetrically cooled spheres. Time and temperature dependence of the coefficient of viscosity and temperature dependence of the coefficient of expansion are included in the theory. The equations are applied to the calculation of quenching stress in glass spheres, and the results are compared with the stress obtained from photoelastic experiments.

Retarded elasticity is neglected in the present theory. The possible errors introduced as a result of this omission are estimated, on the basis of the meager data available, to be less than 20%.

It is also shown that the phenomenon of retarded elasticity can be attributed to macroscopic chemical inhomogeneities known to exist in glass.

Introduction

A mathematical theory of quenching stress in glass and a new photo-elastic technique were recently described by O'Rourke and Saenz[1]. The photoelastic technique was subsequently employed by Parsons[2,3]. His experiments reveal large discrepancies between the stress predicted by O'Rourke's and Saenz' mathematical theory, and that determined by the photoelastic method. It is believed that the main source of these discrepancies is an oversimplified model of the quenching process on which O'Rourke's and Saenz' mathematical theory was based. The latter theory and Parsons' experiments are discussed in Sections I and II.

The viscoelastic behavior of glass, that is included in the present equations, namely, instantaneous elasticity and flow, is discussed in Section III. The equations themselves are derived in Sections IV to VII.

Some of the recent data available on retarded elasticity in glass are described in Section VIII. It is shown that a number of mechanical phenomena exhibited by glass, namely, retarded elasticity, delayed fracture, and a peculiar fracture phenomenon described by Bridgman[4], can be attributed to macroscopic chemical inhomogeneities known to exist in glass.

There are presently too few experimental data available on retarded elasticity in glass to include it in a theory of residual stress. The possible errors introduced in the present calculations as a result of neglecting retarded elasticity, are discussed at the end of Section VIII.

---

[1] R. C. O'Rourke and A. W. Saenz, "Quenching Stresses in Transparent Isotropic Media and the Photoelastic Method," Quart. Appl. Math. **8**, 303-311 (1950).

[2] K. A. Parsons, "A Photoelastic Investigation of Quenching Stresses in Glass," Proc. Soc. Exp. Stress Analysis **10**, No. 1, 1-6 (1952).

[3] K. A. Parsons, "Photoelastic Studies of Quenched Cylinders and Spheres," J. Appl. Phys. **24**, 469-472 (1953).

[4] P. W. Bridgman, "The Effect of Hydrostatic Pressure on the Fracture of Brittle Substances," J. Appl. Phys. **18**, 246-258 (1947).

I. Discussion of Previous Mathematical Theory

Residual stress in glass was recently studied by O'Rourke and Saenz[1], who describe both a mathematical theory and a new photoelastic technique to determine quenching stress in glass. Their mathematical theory consists essentially in simplifying the problem of quenching stress in glass speci-mens to the problem of thermal stress in elastic specimens of the same shape. O'Rourke and Saenz noted that, as the temperature decreases in the annealing range, glass passes rapidly from a nearly fluid to a nearly elas-tic state. They assumed accordingly that a critical temperature T^* may be specified, above which glass is so fluid that it can support only a negligible deviatoric stress, and below which it is nearly elastic. They concluded, that it follows from this assumption, that only a small stress is introduced by quenching a body from a uniform temperature T_o in a bath of temperature T_f , where $T_o > T^* > T_f$, as long as any portion of it is at a temperature above T^* . This stress is neglected in their theory. It is thus actually assumed that prior to a time t^* , where t^* is the time measured from the initial epoch of quenching to the instant the maximum temperature in the en-tire body is T^* , no stress is introduced as a result of quenching. This is in effect to assume that all points of the body pass from a fluid to an elastic state simultaneously at t^* . Accordingly, at t^* one is left with an elastic body free of stress, but with a non-uniform temperature distribu-tion. As time approaches infinity, and thermal equilibrium is attained, a residual stress appears as a result of removing the temperature gradient at t^* . This stress may be calculated from the thermo-elastic equations.

The theory has two major sources of error. First, O'Rourke and Saenz ignore the fact that points near the surface reach the critical temperature T^* much earlier than points inside the body, i.e., that the "freezing"

starts on the surface and proceeds towards the interior. During this period of "freezing" an inhomogeneous thermal contraction of the body takes place, which generally causes a large stress in the exterior after this part of the body becomes elastic, and some hydrostatic stress in the interior, which is still fluid. At t^*, when the whole body has become elastic, the stress is generally large and cannot be neglected in comparison with the final residual stress. The kind of discrepancy introduced as a result of this circumstance is discussed here in the case of quenched spheres.

We distinguish between the idealized fluid-elastic body, which O'Rourke and Saenz postulated, and an idealized fluid-elastic medium, in which the transition from fluid to elastic solid is a property of an element of the body rather than of the body as a whole. The expression for the quenching stress in the idealized medium, when the process of progressive freezing is taken into account, is derived in Section VII, (Equation (7.3)), for the case of a sphere symmetrically quenched. It is shown in Section VII that the deviatoric quenching stress predicted by Equation (7.3) is much higher, particularly near the surface, than that predicted by O'Rourke's and Saenz' theory, when T^* is nearer T_f than T_o. We shall show later that this is the kind of discrepancy that exists between O'Rourke's and Saenz' theory and the results of a photoelastic investigation recently carried out by Parsons[2,3] on quenched glass spheres, where apparently T^* was nearer T_f than T_o.

One notes here that O'Rourke and Saenz made a mathematical error in deriving the expression for the relative retardation predicted by their theory in the case of glass spheres*, and the results shown in Parsons'

---

* Following O'Rourke's and Saenz' instructions to obtain Equation 2.07 from Equation 1.10 in their paper, one finds the relative retardation given by Equation 2.07 to be too large by a factor $\left(\pi/2\right)^{1/2}$.

paper are misleading. In Section VI it is shown also that if T^* is near T_o , O'Rourke's and Saenz' theory predicts much larger deviatoric stress near the surface than Equation (7.3). In the limit as T^* approaches T_o , with $T_o - T_f$ remaining constant, O'Rourke's and Saenz' theory predicts the maximum quenching stress. This apparently is incorrect, because in the limit as T^* approaches T_o the body becomes elastic throughout the quenching process, and no residual stress would result. Hence, O'Rourke's and Saenz' theory predicts too large a stress when T^* is near T_c , and too small a stress when T^* is near T_f .

The second source of error lies in the simplified model of the behavior of glass, which effectively neglects stress above T^* and release of stress below T^*. One is also confronted with the problem of choosing a suitable value of T^*. O'Rourke's and Saenz' theory does not provide any means for calculating this critical temperature from the physical properties of the glass, and it cannot be determined accurately from the physical properties of glass alone, since T^* apparently may be any temperature between the strain point** and some temperature in the annealing range. For lime glass it means that T^* may be any temperature in an interval of at least 50^oC. Now, the magnitude of the residual stress predicted is nearly proportional to $T^* - T_f$, and therefore O'Rourke's and Saenz' theory cannot predict it except when $T^* - T_f \gg 50^o$C, which is generally not the case.

We conclude that, on account of (1) neglect of stress at t^* , which is, in effect, to assume that the whole body "freezes" simultaneously; and (2) lack of accurate means to determine the value of T^*, O'Rourke's and Saenz' theory cannot in general predict the quenching stress in glass. Both

---

** The strain point is the temperature below which no residual stress results from rapid cooling.

of these defects are avoided, in the theory developed below, by introducing
a temperature and time dependent viscous property of the medium.

II. Discussion of Previous Experiments

The new photoelastic technique, described by O'Rourke and Saenz, permits the determination of three dimensional states of stress from measurements of the integrated optical effects after passage of light rays through the specimen. The technique is limited to the study of (1) radially symmetric stress in a sphere and (2) an axially symmetric stress in a cylinder where the sum of the principal stresses equals twice the principal stress in the axial direction. It is not known that axially symmetric quenching stress in a glass cylinder is of the special kind to which the technique applies, and hence, as far as quenching stress is concerned, the technique is limited to the study of radially symmetric stress in a sphere.*** The use of the technique depends, of course, on the knowledge of the stress optical law. At room temperature the birefringence in glass arises from instantaneous elasticity, since glass exhibits essentially only instantaneous elasticity at such low temperatures. At the high temperatures, however, at which the quenching stress is introduced, glass exhibits also retarded elasticity. Thus in a quenched specimen there might be two types of residual stress, namely, an instantaneous elastic stress and a retarded elastic stress, and there are therefore two possible sources of birefringence. The birefringence due to retarded elasticity may be studied separately. From the

---

*** This restriction was recently removed by D. C. Drucker and W. B. Woodward, "Interpretation of Photoelastic Transmission Patterns for a Three-Dimensional Model," J. Appl. Phys. 25, 510-512 (1954).

experimental data available on retarded elasticity in glass it appears that the relaxation time of the phenomenon at room temperature is so large that a retarded elastic stress is practically "frozen". The instantaneous elastic stress in a quenched specimen may then be relieved, without disturbing the "frozen" stress, by cutting the specimen into sufficiently small pieces. The birefringence arising from the retarded elastic stress may thus be determined separately from measurements on the small pieces of glass. Such measurements were made by the author on pieces of glass taken from a quenched sphere, used earlier by Parsons, which the latter was kind enough to make available. Only a small amount of relative retardation, about 150 Å per cm, was observed in specimens taken from near the surface of the sphere. This is quite small compared to the retardation near the surface of the unbroken spheres, which is of the order of 3,000 to 30,000 Å per cm according to Parsons' experiments. The measurements thus indicate that the birefringence, observed by Parsons, in this case was primarily the result of an instantaneous elastic state of stress. It is likely, therefore, that the stress optical coefficient for glass strained at room temperature applies, and the technique described by O'Rourke and Saenz may then be used to determine the instantaneous elastic quenching stress. This can be verified indirectly by comparing the stress thus predicted with the result of an independent theory. With this purpose in mind Parsons compared the measured relative retardation in quenched glass spheres with the retardation predicted from O'Rourke's and Saenz' theory. It is believed here that Parsons did not succeed in justifying the use of the new photoelastic technique to determine quenching stress in glass, for reasons which appear in the following discussion. As mentioned earlier, O'Rourke and Saenz made a mathematical error, and the computed photoelastic curve shown by Parsons is too large by a factor of $\left(\pi^{3}/2\right)^{1/2}$ or about 4. It turns out also that the average value of the coefficient of

expansion used by Parsons is too small by a factor of about 2. Furthermore, Parsons did not use O'Rourke's and Saenz' theory to verify the experimental results, but actually used the latter results to determine a suitable value of T^*, such that the theory and the experiments agree quantitatively. And thus clearly the quantitative agreement obtained does not, as implied by Parsons, justify the use of the photoelastic method. Furthermore, as explained below, it appears that the residual stress observed in some cases was not due to quenching, but was almost entirely a result of the subsequent cooling to room temperature. The composition of the glass has been determined by analysis to be 72.56 per cent SiO_2, 6.39 per cent CaO, and 21.05 per cent Na_2O. An "annealing point" defined by Littleton and Roberts[5] has been determined to be about 500°C for this glass. At this temperature a residual stress in glass is annealed in about fifteen minutes. According to rough calculations, used commercially to calculate annealing schedules, this "annealing time" decreases by a factor of about 2 for each 10°C increase in the temperature. One finds accordingly that at 523°C and 491°C the glass used by Parsons anneals in about three and thirty minutes respectively. The quenched spheres, Nos. 6 and 5, were left in the quenching bath at these temperatures respectively for about fifteen minutes after attaining nearly a thermal equilibrium. One concludes, therefore, that practically no stress can have been present in sphere No. 6 at the end of the quenching process, and the large stress observed by Parsons must have been the result of the subsequent cooling to room temperature. One may note that a cooling of the surface of about 1°C per minute would have produced the observed stress in this case. As to the stress observed in sphere No. 5, it is likely

_____

[5] See G. W. Morey, The Properties of Glass (Reinhold Publ. Corp., New York, 1938) p. 191.

to have been a result both of the quenching to 491°C and the subsequent cooling to room temperature. The agreement obtained by Parsons between theory and experiments in the case of spheres Nos. 5 and 6 is thus misleading. The "strain point" of the glass, as defined by Littleton and Roberts[5], has been determined to be about 470°C. Thus in sphere No. 4, quenched to 450°C, the stress observed must have been practically a result of the quenching only. The comparison in this case between theory and experiment is shown in Fig. 4. One concludes that, even if the quenching experiments had been carried out correctly, Parsons could not successfully have fulfilled the purpose of his investigation, namely, to justify the use of the photoelastic technique in the case of quenching stress by comparing the results with those of an independent theory, since, as explained earlier, O'Rourke's and Saenz' mathematical theory does not predict the quenching stress in glass.

III. Viscoelastic Properties of Lime Glass

There is at present a general agreement among investigators that glass is a viscoelastic medium exhibiting all the important viscoelastic phenomena, namely, instantaneous elasticity, retarded elasticity, and flow. Except, possibly, for retarded elasticity, the viscoelasticity is linear for small strains. Some of the latest data on the viscoelastic properties of lime glass are discussed in this section to arrive at a mechanical model describing approximately the viscoelastic behavior.

The flow in lime glass was recently investigated by Lillie[6]. He found that the viscosity of glass does not depend on the temperature only, but also

---

[6] H. R. Lillie, "Viscosity-Time-Temperature Relations in Glass at Annealing Temperatures," J. Am. Ceram. Soc. 16, 619 (1933).

on the thermal history. The viscosity of glass held at a constant tempera-
ture generally changes with time, and gradually approaches a definite value.
Once this value is attained no further change in the viscosity takes place
at a constant temperature. Lillie called this value the equilibrium vis-
cosity. It depends on the temperature only. He experimented with chilled
fibers subsequently held at a constant temperature. The fibers were quite
thin, and thermal equilibrium was reached almost immediately. Thus the
change in the viscosity could be studied at constant uniform temperature
subsequent to a temperature drop. At first, the coefficient of viscosity,
η , was found to be much lower than the equilibrium viscosity, η_∞ , but
increased gradually and approached η_∞ at a rate given by

$$\frac{d\eta}{dt} = \frac{K_2(\eta_\infty - \eta)}{\eta} \tag{3.1}$$

where K_2 is a constant varying somewhat with the temperature. It has been
argued later by some observers that the change of the viscosity observed
by Lillie may have been merely a result of retarded elasticity. The latter
phenomenon would manifest itself in Lillie's experiments by an apparent
decrease in the viscosity with time. However, Lillie showed also that, in
fibers subjected to a sudden temperature increase, the viscosity was first
higher than η_∞ , and then, with time, approached it from above. This
decrease in viscosity cannot be explained to be a result of retarded elastic-
ity. It is now generally accepted that the viscosity depends on the thermal
history. Since Lillie did not take the effects of retarded elasticity into
account, it is possible that his results are somewhat erroneous. But at
the present time Lillie's empirical formula is the best one available to
describe this phenomenon.

The equilibrium viscosity in glass is extremely sensitive to tempera-
ture. In the annealing range $\log \eta_\infty$ is nearly linearly related to the

temperature. For lime glass this relation is such that η_∞ doubles for every 7.5°C drop in temperature. In Parsons' experiment on sphere No. 4 the temperature drop due to quenching is of the order of 150°C. The corresponding change in the equilibrium viscosity is more than one million fold. The actual viscosity changes somewhat less. According to Lillie's formula (3.1) the change in η is about one hundred thousand fold during the quenching process. The medium thus passes from a nearly fluid to a nearly elastic state. That is, η passes from a value much smaller than η_1 to a value much larger than η_2, where η_1 is the value below which only a negligible amount of deviatoric stress exists under the strain rates encountered, and η_2 is the value above which only a negligible amount of viscous flow takes place under the time and stress encountered. The values of η_1 and η_2 correspond approximately to the equilibrium viscosity at the upper and lower temperatures of the annealing range. The annealing range of the glass used by Parsons is about 470°C to 520°C. The formulae used in this paper to calculate η determine it accurately only in the neighborhood of the interval (η_1 , η_2), and are thus good only for the present purpose.

The equilibrium viscosity of the glass used by Parsons has here been determined from viscosity data due to Lillie[7]. Lillie measured the equilibrium viscosity of three glasses, one of which, denoted glass III, had the composition 71.95 per cent SiO_2, 6.78 per cent CaO, and 20.77 per cent Na_2O. This glass is almost of the same composition as the glass used by Parsons, and from isokoms worked out by Stodt[8] it appears that the viscosity of the two glasses would be nearly the same. The equilibrium viscosity, the

---

[7] H. R. Lillie, "Viscosity of Glass Between the Strain Point and Melting Temperature," J. Am. Ceram. Soc. 14, 502 (1931).

[8] See G. W. Morey, The Properties of Glass (Reinhold Publ. Corp., New York, 1938) p. 159.

"annealing" and "strain point" determined by Lillie for glass III are there-fore used here for Parsons' glass.

The instantaneous elastic behavior of glass in the annealing range has been studied quite extensively, but no conclusive data seem to be available for glass of composition nearly the same as that used by Parsons. However, there seems to be a general agreement that the instantaneous elastic constants of ordinary glasses are quite insensitive to changes in the temperature, albeit they appear generally to decrease slightly with increasing temperature. The temperature dependence of the elastic constants is neglected in the present theory and an average value of the constants is used in the calculations.

Glass exhibits also retarded elasticity. This phenomenon is not included in the present computations, and the subject is therefore deferred to a later section.

In the present paper the viscoelastic behavior of glass is assumed to be that of a Maxwell body, with temperature insensitive elastic constants, and with time and temperature dependent coefficient of viscosity. The stress-strain relation of such a medium is derived in the following section.

IV. Stress-Strain Relation

Fig. 1 shows the mechanical model of the medium. The spring rep-resents the instantaneous, linear, isotropic elasticity of the medium with Young's modulus, E , and Poisson's ratio, ν . The dash-pot represents incompressible Newtonian flow, characterized by the viscosity coefficient η . E and ν are assumed to be constant, and η to be a function of time and temperature.

The equilibrium of the model requires that the stress in both elements be equal. The stress-strain relation for the elastic element is

$$\underset{\sim}{\epsilon}_1 = \frac{1+\nu}{E} \underset{\sim}{\sigma} - \frac{\nu}{E} \underset{\sim}{\sigma} : \underset{\sim}{I} \; \underset{\sim}{I} \tag{4.1}$$

where $\underset{\sim}{\epsilon}_1$, $\underset{\sim}{\sigma}$, and $\underset{\sim}{I}$ are the elastic pure strain dyadic*, the stress dyadic, and the idem factor respectively.

For the flow element we have

$$\frac{\partial \underset{\sim}{\epsilon}_2}{\partial t} = \frac{1}{2\eta} \underset{\sim}{\tau} \tag{4.2}$$

where $\underset{\sim}{\epsilon}_2$ and $\underset{\sim}{\tau}$ are the viscous pure strain dyadic and the deviatoric stress dyadic respectively. That is, the material can flow deviatorically but not volumetrically.

Let α be the coefficient of linear thermal expansion and T the temperature, then the thermal strain is

$$\underset{\sim}{\epsilon}_3 = \epsilon \underset{\sim}{I} \tag{4.3}$$

where $\epsilon = \int^T \alpha \, dT$

Let $\underset{\sim}{\epsilon}$ be the macroscopic pure strain dyadic including the thermal strain of the medium. The geometry of the model requires

$$\underset{\sim}{\epsilon} = \underset{\sim}{\epsilon}_1 + \underset{\sim}{\epsilon}_2 + \underset{\sim}{\epsilon}_3 \tag{4.4}$$

Adding the time derivatives of Equations (4.1) and (4.3) to (4.2) we obtain

$$\frac{\partial \underset{\sim}{\epsilon}}{\partial t} = \frac{1}{2\eta} \underset{\sim}{\tau} + \frac{1+\nu}{E} \frac{\partial \underset{\sim}{\sigma}}{\partial t}$$

$$- \frac{\nu}{E} \frac{\partial \underset{\sim}{\sigma} : \underset{\sim}{I}}{\partial t} \underset{\sim}{I} + \frac{\partial \epsilon}{\partial t} \underset{\sim}{I} \tag{4.5}$$

---

* For the dyadic notation used in this paper, see C. E. Weatherburn, Advanced Vector Analysis (G. Bell and Sons, London, 1928).

-12-

which is the isotropic stress-strain relation of the medium including thermal strain. This relation may conveniently be resolved into two, relating the volumetric and deviatoric parts separately and becomes, then,

$$\frac{\partial \underset{\sim}{\gamma}}{\partial t} = \left(\frac{1}{2\eta} + \frac{1+\nu}{E}\frac{\partial}{\partial t}\right)\underset{\sim}{\tau}$$

$$\frac{\partial \theta}{\partial t} = 3\frac{1-2\nu}{E}\frac{\partial \Theta}{\partial t} + 3\frac{\partial \epsilon}{\partial t}$$

(4.6)

where $\underset{\sim}{\gamma}$ is the deviatoric strain dyadic, θ the cubical dilatation, and Θ the mean tension.

V. Radially Symmetrical Thermal Stress

In the case of radial symmetry, stress and strain may be specified by the radial and tangential components only. Let these components be identified by subscripts r and φ respectively.

The equation of equilibrium in the absence of body forces, $\underset{\sim}{\nabla}\cdot\underset{\sim}{\sigma} = 0$, reduces in this case to

$$\frac{\partial \sigma_r}{\partial r} + \frac{2}{r}\left(\sigma_r - \sigma_\varphi\right) = 0$$

(5.1)

and the equation of compatibility, $\underset{\sim}{\nabla}\times\underset{\sim}{\epsilon}\times\underset{\sim}{\nabla} = 0$, reduces to

$$\frac{\partial \epsilon_\varphi}{\partial r} - \frac{1}{r}\left(\epsilon_r - \epsilon_\varphi\right) = 0$$

(5.2)

One finds that the radial component of the deviatoric stress is given by

$$3\tau_r = 2\left(\sigma_r - \sigma_\varphi\right)$$

(5.3)

Noting also that $\sigma_r = \bar{\tau}_r + \Theta$ Equation (5.1) becomes

$$\frac{\partial \Theta}{\partial r} + \frac{1}{r^3}\frac{\partial}{\partial r}\left(r^3\tau_r\right) = 0$$

(5.4)

-13-

Furthermore the radial component of the deviatoric strain is given by

$$3\gamma_r = 2(\epsilon_r - \epsilon_\varphi)$$

and, also,

$$2\tau_\varphi = -\tau_r, \qquad 3\epsilon_\varphi = 3\gamma_\varphi + \theta$$

With these results and (4.6), the time derivative of (5.2) becomes,

$$-\frac{\partial}{\partial r}\left(D_1[\tfrac{\tau_r}{2}]\right) + \frac{1-2\nu}{E}\frac{\partial^2\theta}{\partial r\partial t}$$

$$+ \frac{\partial^2\epsilon}{\partial r\partial t} - \frac{1}{r}\frac{3}{2}D_1[\tau_r] = 0$$

where

$$D_1 = \left(\frac{1}{2\eta} + \frac{1+\nu}{E}\frac{\partial}{\partial t}\right)$$

which reduces to

$$-\frac{1}{2r^3}\frac{\partial}{\partial r}\left(D_1[r^3\tau_r]\right) + \frac{1-2\nu}{E}\frac{\partial^2\theta}{\partial r\partial t} + \frac{\partial^2\epsilon}{\partial r\partial t} = 0 \qquad (5.5)$$

Eliminating θ between (5.4) and (5.5) we have

$$\frac{1}{r^3}\frac{\partial}{\partial r}\left(D_2[r^3\tau_r]\right) = 4\beta\frac{\partial^2\epsilon}{\partial r\partial t} \qquad (5.6)$$

where

$$D_2 = \left(\frac{\beta}{\eta} + \frac{\partial}{\partial t}\right)$$

and

$$\beta = \frac{E}{6(1-\nu)}$$

Integrating (5.6) with respect to r we have

$$D_2[r^3 \tau_r] = 4\beta \int_a^r \rho^3 \frac{\partial^2 \epsilon(\rho,t)}{\partial \rho \partial t} d\rho + G(t) \tag{5.7}$$

where $G(t)$ is a function of integration. Let

$$H(r,t) = 4\beta \int_a^r \rho^3 \frac{\partial^2 \epsilon(\rho,t)}{\partial \rho \partial t} d\rho + G(t)$$

and

$$\psi(r,t) = \beta \int_0^t \frac{d\lambda}{\eta(r,\lambda)}$$

Then the general solution of (5.7) is

$$\tau_r = r^{-3} e^{-\psi(r,t)} \int_0^t e^{\psi(r,\lambda)} H(r,\lambda) d\lambda + f(r) e^{-\psi(r,t)} \tag{5.8}$$

where $f(r)$, a function of integration, is the initial stress in the medium.

From Equations (5.1) and (5.3) we have

$$\frac{\partial \sigma_r}{\partial r} = -\frac{3}{r} \tau_r$$

$$\sigma_r = 3 \int_r^a \frac{\tau_r(\rho,t)}{\rho} d\rho + \sigma_r \Big|_{r=a} \tag{5.9}$$

and

$$\sigma_\varphi = \sigma_r - \frac{3}{2} \tau_r \tag{5.10}$$

$G(t)$ and $f(r)$ are determined from the initial and boundary conditions, and a is the inner radius of the sphere.

VI. Thermal Stress in a Solid Sphere

Assume that the sphere is solid, of radius b , and is free of stress initially at $t = 0$, that is, $a = 0$ and $f(r)$ in (5.8) is identically zero, and the subsequent stress is due only to a thermal strain ϵ . In order that τ_r be finite at $r = 0$, $G(t)$ must be identically zero. Thus (5.8) becomes

$$\tau_r = 4\beta e^{-\psi(r,t)} \int_0^t e^{\psi(r,\lambda)} \frac{\partial}{\partial \lambda} \left[\frac{1}{r^3} \int_0^r \rho^3 \frac{\partial \epsilon}{\partial \rho} d\rho \right] d\lambda \tag{6.1}$$

and (5.9) and (5.10) become, after using the boundary condition $\sigma_r = 0$ at $r = b$,

$$\sigma_r = 3 \int_r^b \frac{\tau_r(\rho, t)}{\rho} d\rho \tag{6.2}$$

$$\sigma_\varphi = 3 \int_r^b \frac{\tau_r(\rho, t)}{\rho} d\rho - \frac{3}{2} \tau_r \tag{6.3}$$

Integrating the term in brackets in (6.1) by parts we get

$$\tau_r = 4\beta e^{-\psi(r,t)} \int_0^t e^{\psi(r,\lambda)} \frac{\partial}{\partial \lambda} \left[\epsilon(r,\lambda) - \frac{3}{r^3} \int_0^r \epsilon(\rho,\lambda) \rho^2 d\rho \right] d\lambda \tag{6.4}$$

where the term in brackets expresses the difference between the thermal strain at radius r and the average thermal strain within the sphere of radius r . A formula for the thermal stress may now be obtained by inserting (6.4) in (6.2) and (6.3). If we let η be infinitely large, i.e., the body is elastic, (6.4) reduces to

$$\tau_r = 4\beta \left[\epsilon - \frac{3}{r^3} \int_0^r \epsilon \rho^2 d\rho \right] \tag{6.5}$$

and inserting this in (6.2) and (6.3) one obtains

$$\sigma_r = 12\beta\left[\frac{1}{b^3}\int_0^b \in \rho^2 d\rho - \frac{1}{r^3}\int_0^r \in \rho^2 d\rho\right]$$

$$\sigma_\varphi = 12\beta\left[\frac{1}{b^3}\int_0^b \in \rho^2 d\rho + \frac{1}{2r^3}\int_0^r \in \rho^2 d\rho - \frac{\in}{2}\right]$$

which are identical with the well known elastic solution[*], except that the coefficient of expansion is usually assumed constant, i.e., $\in = \propto T$.

VII. Quenching Stress in Glass Spheres

Let a sphere of glass be quenched from a temperature T_o , at which the glass is quite fluid, to a temperature T_f , at which it is nearly solid. It is assumed that the surface temperature initially decreases discontinuously with time from T_o to T_f and remains at T_f during the quenching process. Let T be the temperature measured from T_f . We have then[**]

$$T = 2T_o \sum_{n=1}^\infty (-1)^{n+1} \frac{\sin n\pi\xi}{n\pi\xi} e^{-\frac{n^2 \mathcal{K}\pi^2}{b^2}t} \tag{7.1}$$

where $\mathcal{K}$ is the diffusivity of the medium, b the radius of the sphere, and $\xi = \frac{r}{b}$.

The expression for the radial deviatoric residual stress is obtained by setting $t = \infty$ in (6.4), with the result

$$\tau_r = 4\beta\int_0^\infty \exp\left(-\beta\int_t^\infty \frac{d\lambda}{\eta(r,\lambda)}\right) \frac{\partial}{\partial t}\left[\in - \frac{3}{r^3}\int_0^r \in \rho^2 d\rho\right] dt \tag{7.2}$$

The radial and tangential components of stress may be obtained by inserting Equation (7.2) in (6.2) and (6.3).

---

[*] S. Timoshenko, Theory of Elasticity (McGraw-Hill, New York and London, 1934) p. 377.

[**] W. E. Byerly, Fourier's Series and Spherical Harmonics (Ginn and Co., Boston, 1893) p. 116, example 2.

The expression for the deviatoric quenching stress in the idealized _medium_ may be calculated from Equation (7.2). This equation takes into account the fact that points at different distances from the center of the sphere assume the critical temperature T^* at different times. As mentioned in Section I, this circumstance was ignored by O'Rourke and Saenz. For such a medium one has $\eta = 0$ for $T > T^*$ and $\eta = \infty$ for $T < T^*$, i.e., the medium cannot support any deviatoric stress at temperatures above, and is perfectly elastic at temperatures below T^*. To perform the integration of Equation (7.2) with respect to time, let us assume that the radius is fixed at some arbitrary value, r_0, and let $\bar{t}(r_0)$ be the time measured from the initial epoch of quenching to the instant the temperature at r_0 is T^*. One should note the difference between t^* defined in Section I and $\bar{t}(r_0)$. The latter is a function of the radius, and it equals t^* for $r_0 = 0$. Noting that at $r = r_0$

$$exp\left(-\beta \int_t^\infty \frac{d\lambda}{\eta(r_0,\lambda)}\right) = \begin{cases} 0, & t < \bar{t}(r_0) \\ 1, & t > \bar{t}(r_0) \end{cases}$$

one finds that the integration of Equation (7.2) yields

$$\tau_r\Big|_{r=r_0} = -4\beta\left(\epsilon - \frac{3}{r^3}\int_0^r \epsilon \rho^2 d\rho\right)\Big|_{\substack{r=r_0 \\ t=\bar{t}(r_0)}} \tag{7.3}$$

Comparing Equations (6.5) and (7.3) one finds that the quenching stress in the idealized medium at $r = r_0$ is equal, except for sign, to the thermal stress in an elastic sphere at $r = r_0$, with elastic properties equal to the instantaneous elastic properties of the idealized medium, due to a temperature distribution evaluated from Equation (7.1) at the time $\bar{t}(r_0)$. For the argument in Section I it suffices to assume that the coefficient of expansion is constant. Equation (7.3) may then be written

$$\tau_r\big|_{r=r_o} = -4\beta\alpha\frac{3}{r^3}\int_0^{r_o}\left[T^* - T(\rho, \bar{t}(r_o))\right]\rho^2 d\rho \tag{7.4}$$

while the corresponding stress predicted by O'Rourke's and Saenz' theory is

$$\tau_r\big|_{r=r_o} = -4\beta\alpha\frac{3}{r^3}\int_0^{r_o}\left[T(r_o, t^*) - T(\rho, t^*)\right]\rho^2 d\rho \tag{7.5}$$

In Figs. 2 and 3 the temperature distribution at $t = t^*$ and at $t = \bar{t}(r_o)$ for $r = .8b$ is shown. Equation (7.4) predicts a stress at $r = r_o$ equal to the thermal stress in an elastic body as a result of removing the temperature distribution at $\bar{t}(r_o)$, whereas O'Rourke's and Saenz' theory predicts a stress equal to the thermal stress in an elastic body due to the removal of the temperature distribution at t^*. In Fig. 2, the temperature distributions at $\bar{t}(r_o)$ and t^* are compared in the case when T^* is nearer T_f than it is to T_o, and apparently O'Rourke's and Saenz' theory predicts a much smaller stress than Equation (7.4). In Fig. 3 T^* is near T_o, and in this case O'Rourke's and Saenz' theory predicts much larger stress than Equation (7.4). This is the error introduced in O'Rourke's and Saenz' mathematical theory as a result of the simplifying assumption that all points of the body "freeze" simultaneously.

The radial deviatoric quenching stress may be calculated from Equation (7.2) inserting the actual variation in the physical constants with time and temperature. On account of the resulting complex analytical form of the integrand of Equation (7.2), it can only be integrated numerically. This has been done to predict the quenching stress in sphere No. 4 which was examined by Parsons. The result is shown in Fig. 4. The complete histories of the deviatoric, instantaneous elastic strain and the viscous strain are shown in Fig. 5 for points a distance .8b from the center of sphere No. 4. Since the thermal history of spheres Nos. 5 and 6 is not known during the cooling to room temperature, the stress in these spheres cannot be evaluated by the present theory for reasons explained in Section I.

-19-

The physical constants of the glass used by Parsons have been determined as follows:

The coefficient of expansion has been determined from expansion measurements on the glass used by Parsons. These measurements were carried out at Bell Telephone Laboratories, and the results are shown in Fig. 6. The measurements were carried out only to about 530°C, and the coefficient of expansion above this temperature has been estimated from other experimental results*. The equilibrium viscosity of the present glass is, as mentioned in Section III, nearly equal to the equilibrium viscosity of a glass of about the same chemical composition on which Lillie carried out extensive viscosity measurements. The value used here is

$$\eta_\infty = 10^{33.6 - \frac{T}{25}} \quad \text{poises}$$

and is sufficiently accurate for the present purpose. The variation in the actual viscosity, η , with time has been determined by a numerical integration of Lillie's formula, Equation (3.1). The values of the parameter K_2 used here are as determined by Lillie for a lime glass of a somewhat different chemical composition, having an "annealing point" about 9°C higher than that used by Parsons. The values of the diffusivity, Young's modulus and Poisson's ratio used are as given by Parsons. The values are, respectively,

$$4.67 \cdot 10^{-3} \text{ cm}^2/\text{sec} \quad ; \quad 6.68 \cdot 10^{11} \text{ dynes/cm}^2 \quad ; \quad (.184) \ .$$

The numerical integration of Equation (7.2) with respect to time has been carried out from the initial epoch of quenching, $t = 0$ to the time the sphere was removed from the bath, t = 2700 sec. Due to uncertainties regarding the temperature very near the surface and the thermal history effects

---

* See table XI 12, after Seddon, Turner, and Winks, p. 280 in reference 5.

on the viscosity of glass rapidly cooled, the stress has been evaluated only for values of r/b less than .9.

It turns out that the deviatoric quenching stress near the surface and near the center of the sphere cannot be determined accurately by O'Rourke's and Saenz' photoelastic technique. One notes that the length of the light path, which lies within the medium, decreases rapidly with increasing radius, and the rate of decrease approaches infinity as r approaches b. This makes the determination of the stress near the surface very difficult. Near the center of the sphere one finds that small variations in the integrated relative retardation correspond to very large variations in the deviatoric stress. Since small errors are inherent in the measurements of the relative retardation, the deviatoric stress near the center predicted from Parsons' experiments cannot be considered very accurate.

One notes from Fig. 4 that there is a rather good agreement between the stress predicted by the present theory and Parsons' experiments for sphere No. 4. The agreement suggests that both the new photoelastic technique described by O'Rourke and Saenz and the present theory predict the instantaneous elastic quenching stress in glass. The stress predicted by O'Rourke's and Saenz' theory is also shown in Fig. 4, using $T^* = 500^{\circ}C$, which is the "annealing temperature" of the medium. One notes that the predicted deviatoric stress is much too small near the surface.

VIII. Retarded Elasticity in Glass

There is sufficient experimental evidence available at the present time to demonstrate the presence of retarded elasticity in ordinary glass. There is, however, no agreement among observers about the physical constants characterizing the phenomenon, namely, the relaxation time and the elastic

constants associated with it. Retarded elasticity was investigated recently
in lime glass at temperatures between the strain point and the softening
point by Taylor and co-workers[9]. They measured the deformation of fibers
at constant temperature subsequent to the application and removal of loads.
The fibers were held at constant temperature sufficiently long before each
experimental run so that the equilibrium viscosity was essentially attained.
The deformation due to irreversible viscous flow thus proceeded at a con-
stant rate, depending on the load only, at each temperature. It could then
be accurately subtracted from the total deformation, and the reversible
viscoelastic deflection could be studied separately. This deflection con-
sists of two parts, an instantaneous elastic and a retarded elastic deflec-
tion. To distinguish between these phenomena Taylor measured the deforma-
tion of the fibers just before and five seconds after the application and
removal of loads, and attributed the change in the reversible deformation
between these epochs to instantaneous elasticity. It was later pointed out
by Jones[10,11,12] that some retarded elastic deformation occurred within
these five seconds, particularly at higher temperatures, since the retarded
elastic strain rate is then quite rapid, and that Taylor therefore failed
to separate the instantaneous elastic and retarded elastic strains. Jones

[9] N. W. Taylor, E. P. McNamara, J. Sherman, "A Study of the Elastico-
Viscous Properties of a Soda-Lime-Silica Glass at Temperatures near the
"Transformation Point"," J. Soc. Glass Tech. 21, 61 (1937).

[10] G. O. Jones, "The Determination of the Elastic and Viscous Properties
of Glass of Temperatures below the Annealing Range," J. Soc. Glass Tech.
28, 432 (1944).

[11] G. O. Jones, "The Influence of Delayed Elasticity on the Rate of
Annealing of Glass," J. Soc. Glass Tech. 31, 218 (1947).

[12] G. O. Jones, "Some Aspects of the Flow Properties of Glass of Very
High Viscosity," J. Soc. Glass Tech. 33, 64 (1949).

concluded thus that the variation in the magnitude of the retarded elastic
strain with temperature, determined by Taylor to be decreasing with increas-
ing temperature, is incorrect. One notes here that variation with tempera-
ture of the retarded elastic strain can be determined approximately from
Taylor's values of the total reversible deflection, which are quite reliable,
and data available on instantaneous elasticity in glass*. First, Taylor
found that the total reversible strain does not vary with the temperature
in the annealing range. Secondly, the results of data, just referred to,
indicate that the instantaneous elastic deflection is quite insensitive to
the temperature, however, increasing somewhat with the temperature. There-
fore, we may conclude that the retarded elastic strain, being the difference
between the former two, must also be quite insensitive to changes in the
temperature near the annealing point, decreasing somewhat with temperature.
It appears then from Taylor's experiments that the magnitude of the retarded
strain is somewhat smaller than the corresponding instantaneous elastic
strain. Taylor studied also the relaxation time of the phenomenon, and he
found that it is nearly proportional to the equilibrium viscosity of the
glass. If we extrapolate the values of the relaxation time, we find that
at lower temperatures the phenomenon cannot be observed unless experimental
runs are carried out for many months or years. This has not yet been done.
Short time observations, however, were carried out by Jones[10,11,12] at tem-
peratures ranging from about 200°C to the annealing point, about 520°C.
He found that below 400°C there is a small amount of retarded elastic defor-
mation, of the order of five per cent of the corresponding instantaneous
elastic deformation, with much shorter relaxation time than that predicted
from extrapolations of Taylor's results. The difference in the relaxation

_____

* See reference 5, pp. 307-314.

-23-

times is apparently of many orders of magnitude. At about 400°C Jones observed an increase in the retarded deformation to about seventy per cent of the corresponding instantaneous elastic strain. Jones' results indicate that the magnitude of the retarded deformation is insensitive to temperature above 400°C, which agrees with the conclusion arrived at above, on the basis of Taylor's values of the total reversible strain and the data, referred to, on the instantaneous elastic strain. Jones, however, did not believe his results to be reliable at temperatures much above 400°C. On the basis of the rapid increase in the deformation observed at about 400°C, he conjectured that it would continue to increase rapidly in the annealing range, becoming much larger than the instantaneous elastic deflection at higher temperatures. One notes here, that Jones obtained no direct experimental evidence of such a continued increase of the retarded deformation in the annealing range, and the conclusion arrived at earlier, namely, that the magnitude of the retarded deformation is rather insensitive to the temperature, seems to be more reliable.

If glass exhibits a large retarded deformation also at lower temperatures, one notes that Jones would not have been able to observe it in his short time experiments, since, as indicated by Taylor's results, the relaxation time of the phenomenon would be extremely large. It is quite likely that the small deformation measured by Jones is only the initial rapid development of the retarded deformation at lower temperatures, and that actually a much larger retarded strain exists with very long relaxation time.

This is just the kind of retarded elasticity one would expect to be exhibited by glass as a result of inhomogeneities in the chemical composition which are known to exist in glass. The viscosity of glass is extremely sensitive to small variations in the composition, and thus glass is an inhomogeneous viscoelastic medium, having essentially a space dependent viscosity.

-24-

The inhomogeneity in the density of glass was recently studied by J. C. Turnbull[13], and F. V. Tooley and R. L. Tiede[14,15]. Their experiments show that quite large variations in the density exist, apparently on a small scale comparable to the grain size of the raw materials used. The variation in density is known to be a result of a variation of the chemical composition, but very few data are yet available to correlate the spread in density, observed in these experiments, with a spread in the chemical composition. Judging from the few data available, however, spreads in the chemical composition corresponding to more than ten per cent variations in the major ingredients are likely to exist in glass. This corresponds to more than a thousand fold spread in the coefficient of viscosity. Thus glass seems to be composed of a large number of small regions each having different viscosity. From Tooley's and Tiede's experiments it appears that only a small fraction of the glass was found to have a density very much different from the average, and hence it would seem that only a small fraction of the glass would have a viscosity differing from the average by factors of more than a thousand, and that the viscosity of the remaining glass would vary within narrower limits. Nothing is presently known about the shape of these regions, which might largely determine the overall mechanical behavior of the medium. It is, therefore, not yet possible in general to predict the overall viscoelastic behavior of glass as a consequence of inhomogeneities. In the fibers used by Taylor, however, these regions must

---

[13] J. C. Turnbull, "Separation of Inhomogeneities in Bottle Glass by Density Differences," J. Am. Ceram. Soc. 24, 37 (1941).

[14] F. V. Tooley and R. L. Tiede, "Factors Affecting the Degree of Homogeneity of Glass," J. Am. Ceram. Soc. 27, 42 (1944).

[15] R. L. Tiede and F. V. Tooley, "Effect of Temperature on Homogenizing Rate of Soda-Lime-Silica Glass," J. Am. Ceram. Soc. 28, 42 (1945).

have been very much elongated along the axis of the fiber, due to the very large viscous flow in this direction as the fibers were drawn. For the same reason, in the glass plates used by Jones, the regions must have been elongated in the plane of the plates. This is not the case for the small, stiffer portions of the glass, which would likely still have small dimensions in all directions. In both the fibers and the plates then, the regions of intermediate and low viscosity would be very much elongated in the direction of the applied stress. They would then act together like, for example, the fibers in textiles, and would be subjected to nearly the same elongation under the stress. The regions of higher viscosity would have much less effect on the overall behavior of such a medium, being more or less spherical in shape and not connected with each other. If it is assumed that homogeneous glass exhibits instantaneous elasticity and flow only, which is generally the case of solid solutions, one would predict that the behavior observed by Jones and Taylor can be represented by a mechanical model consisting of a number of Maxwell elements arranged in parallel, the elements having nearly the same elastic constants but quite different coefficients of viscosity. This is, indeed, the case. Such a mechanical model is shown in Fig. 7. The elements are assumed to be arranged in the order of decreasing viscosity. The few elements of low viscosity represent the smaller but most fluid portion of the glass, and the elements of intermediate viscosity represent the major portion of the glass. The elements corresponding to the regions of high viscosity are left out, since their effect on the overall behavior would be small for the reasons mentioned above. The elements of low viscosity account for the initial rapid relaxation of the retarded strain, which was observed by Jones. At low temperatures the elements of intermediate relaxation times, which represent the major portion of the glass, would exhibit essentially instantaneous elasticity only during short

time loading, and the smaller, more viscous part of the medium, represented by the low viscosity elements, would give rise to a small amount of retarded deformation with short relaxation time. As the temperature increases, a continually larger part of the glass would flow appreciably under short time loading, and the medium would appear to exhibit an increasingly larger retarded strain. This agrees with the actual observations described by Jones. At high temperatures the initial rate of relaxation of the retarded strain would be extremely fast, because the relaxation time of the low viscosity elements then would be extremely short The magnitude of this initial, rapid, retarded strain, however, would be quite small compared to the retarded strain caused by the elements of the intermediate relaxation times, which represent the larger portion of the glass. Taylor must have failed to observe the small amount of retarded elasticity which is developed quite rapidly initially. He observed apparently only the larger amount of retarded elasticity exhibited by the larger portion of the glass, and which at high temperatures has a sufficiently short relaxation time so that it may be studied under short time loading.

It turns out that the derivative of $\log \eta$ with respect to temperature is insensitive to variations in the chemical composition, and it is nearly constant in the annealing range and at temperatures below*. It follows, since the dash-pots in Fig. 7 represent the viscosities of glasses of slightly different compositions, that the ratios of the viscosities of these elements are insensitive to the temperature. One finds, therefore, that the magnitude of the retarded deformation predicted by the model in Fig. 7 is insensitive to the temperature, and that the relaxation time of the phenomenon is proportional to the average viscosity of the irreversible

---

* See Figure V 10, due to S. English, in reference 5, p. 150.

-27-

flow of the medium. These predictions agree with the conclusions arrived at earlier on the basis of Taylor's experiments and the data, referred to, on instantaneous elasticity in glass. The retarded deformation predicted from Fig. 7 is in good agreement with the experimental observations of Taylor and Jones, and it is concluded, therefore, that the phenomenon of retarded elasticity in glass can be attributed to chemical inhomogeneities in glass.

One may note that the magnitude and the relaxation time of the phenomenon, determined by Taylor and Jones, are not in general applicable to glass specimens of the same composition, but of shapes other than fibers or plates, because, as explained earlier, the overall behavior is likely to depend to a large extent on both the shape of the regions of different composition, and possibly also on the degree of homogeneity. One notes also that both glass fibers and plates are likely anisotropic, and would exhibit different amounts of retarded elasticity depending on the direction of the applied stress. Glass which has not been subjected to large viscous flow in any particular direction, might be expected to be statistically isotropic and would possibly exhibit less retarded elasticity.

It might be mentioned here that a number of mechanical phenomena exhibited by glass, for example, delayed fracture, fracture under hydrostatic pressure with the pressure reduced in one direction[4], and possibly also the increased strength of fibers, may be explained as a result of chemical inhomogeneities. One would expect, namely, that initially, when a piece of glass is loaded, the stress would be uniformly distributed, because the elastic constants are rather uniform. With time, however, the stress in the more viscous regions would relax partly, and the stress would be transferred to the stiffer regions in the medium. This would lead to concentrations of stress, which would initiate small fractures. The small

fractures would then propagate, and lead to complete fracture of the body. In fibers, where the regions of different viscosity are elongated in the direction of the stress, the stress concentration is known from the theory of elasticity to have less effect, and therefore one would expect the fibers to be stronger. One would, in general, predict that glass, subjected to long time loading, is strongest in the directions in which a large viscous flow has taken place.

In order to estimate the possible errors introduced in the present calculations of the instantaneous elastic quenching stress as a result of neglecting retarded elasticity, it is convenient first to study the history of the quenching process predicted by the present theory. In Fig. 5 the variation with time of the instantaneous elastic strain and the viscous flow is shown for sphere No. 4 at $r = .8b$ from the initial epoch of quenching to the time the sphere was removed from the bath. The figure serves here to illustrate the important phenomena of the quenching process. Confining our attention to a shell of infinitesimal thickness at a fixed value of the radius, one may distinguish between the following two stages of the quenching process:

(i) At times $t < 200$ sec., the thermal contraction of the shell is much more rapid than the average thermal contraction of the interior. A large viscous stretch of the shell takes place, and practically no instantaneous elastic deviatoric strain exists, because the shell is yet too fluid to support deviatoric stress.

(ii) At times $t > 200$ sec., the thermal contraction of the shell is gradually becoming slower than the average thermal contraction of the interior. A viscous flow now takes place in the opposite direction, and as the shell becomes stiffer, a compressive instantaneous deviatoric strain is gradually introduced.

-29-

One notes here that the deviatoric stress in the case of a sphere depends on the viscosity only at the particular value of the radius at which it is evaluated. This is clear from Equation (7.2) noting that in the time integration, which yields the deviatoric stress, the value of the radius is held fixed. This would be the case even if the medium exhibits, in addition to instantaneous elasticity and incompressible flow, also incompressible retarded elasticity. It can be shown, namely, by a simple symmetry argument that the deviatoric stress at any r_0 depends on the compressibility of the medium at $r < r_0$ and the elastic and viscous properties of the medium at $r = r_0$. One assumes here that both the reversible and irreversible flows are deviatoric only, and hence have no effect on the dilatation of the medium. It follows then that in the first stage of the quenching process, described earlier, the effect of retarded elasticity must necessarily be small because the shell is too fluid to support any deviatoric stress. The irreversible flow dominates during this stage of the quenching process. A retarded elastic stress, however, will be introduced during the second stage, and is accompanied by an elastically retarded flow in the same direction as the irreversible flow. Thus, the apparent coefficient of viscosity of the shell during the second stage of the quenching process will at all times be lower than the coefficient of viscosity of the irreversible flow. The total flow, i.e., the sum of the reversible and irreversible flow, would thus be larger during the second stage of the quenching process, than the flow predicted by the present theory. Hence, the present theory would be likely to predict too large instantaneous elastic deviatoric stress.

According to Taylor's results the apparent viscosity of glass, subsequent to loading, varies between about $.8\eta$ and η, where η is the coefficient of viscosity of the irreversible flow. Assuming that this is

the case., the instantaneous elastic deviatoric stress would apparently lie between the value predicted by the present theory and the smaller value obtained inserting $.8\eta$ in Equation (6.2). The latter value is about 20 per cent lower than the stress shown in Fig. 4. This is then a very rough estimate of the error introduced as a result of neglecting retarded elasticity.
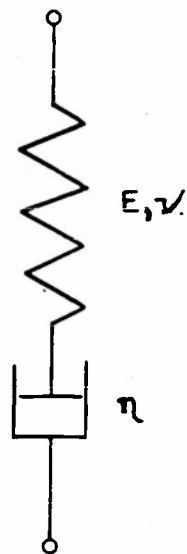
Acknowledgment

Fig. 1

The mechanical model of the idealized viscoelastic medium.

Fig. 2

The temperature distribution in a sphere at times $t = \bar{t}(r_o)$ and $t = t^*$, when T^* is nearer T_o than T_f. The deviatoric stresses at $r = .8b$ predicted by O'Rourke's and Saenz' theory and Equation (7.3) are proportional to the shaded and cross hatched areas respectively.
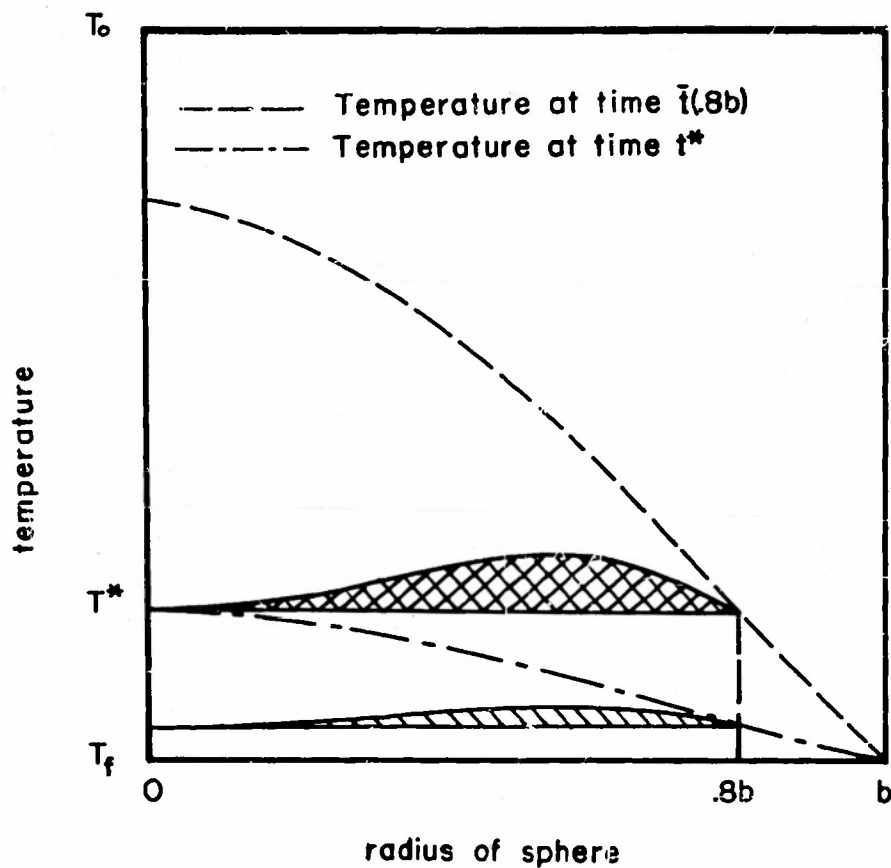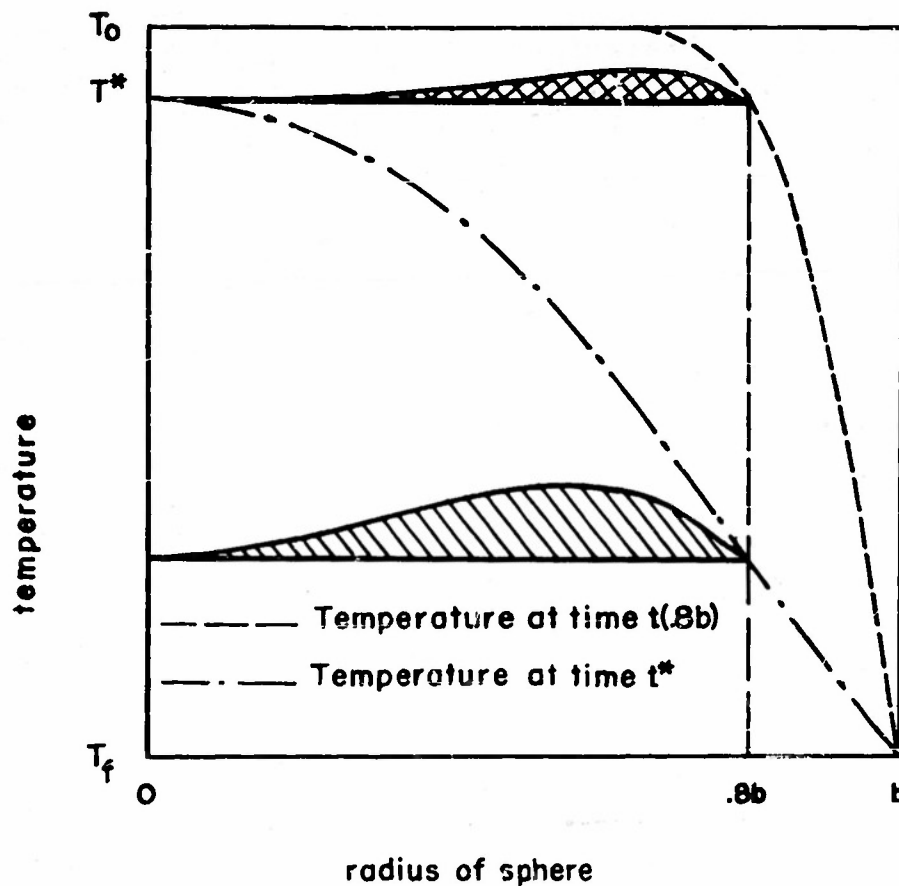
Fig. 3

The temperature distribution in a sphere at times $t = t(r_0)$ and $t = t^*$, when T^* is nearer T_f than T_0. The deviatoric stresses at $r = .8b$ predicted by O'Rourke's and Saenz' theory and Equation (7.3) are proportional to the shaded and cross hatched areas respectively.
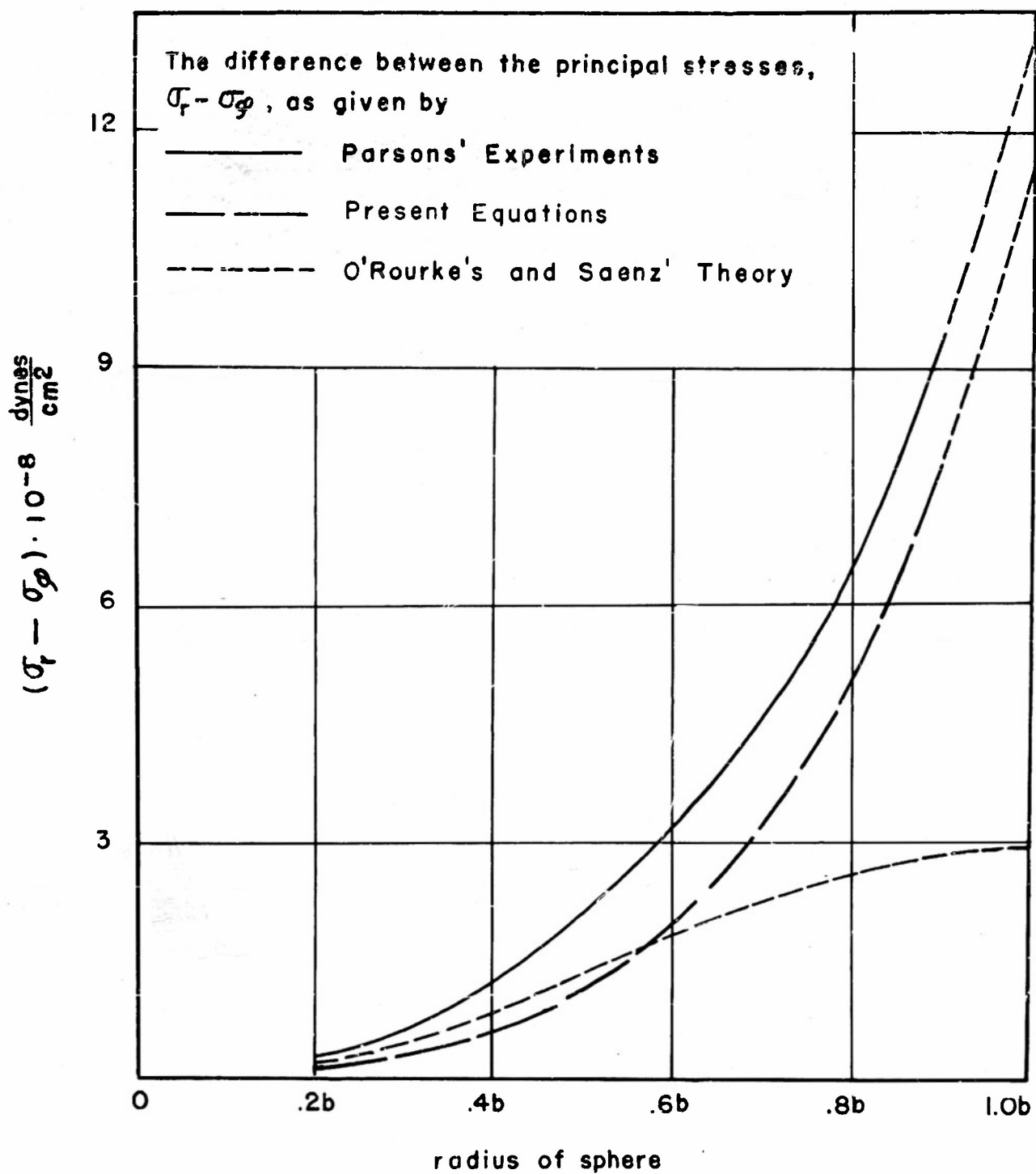
Fig. 4

The difference between the principal stresses in
sphere No. 4 as given by Parsons' experiments, the
present equations, and O'Rourke's and Saenz' theory.
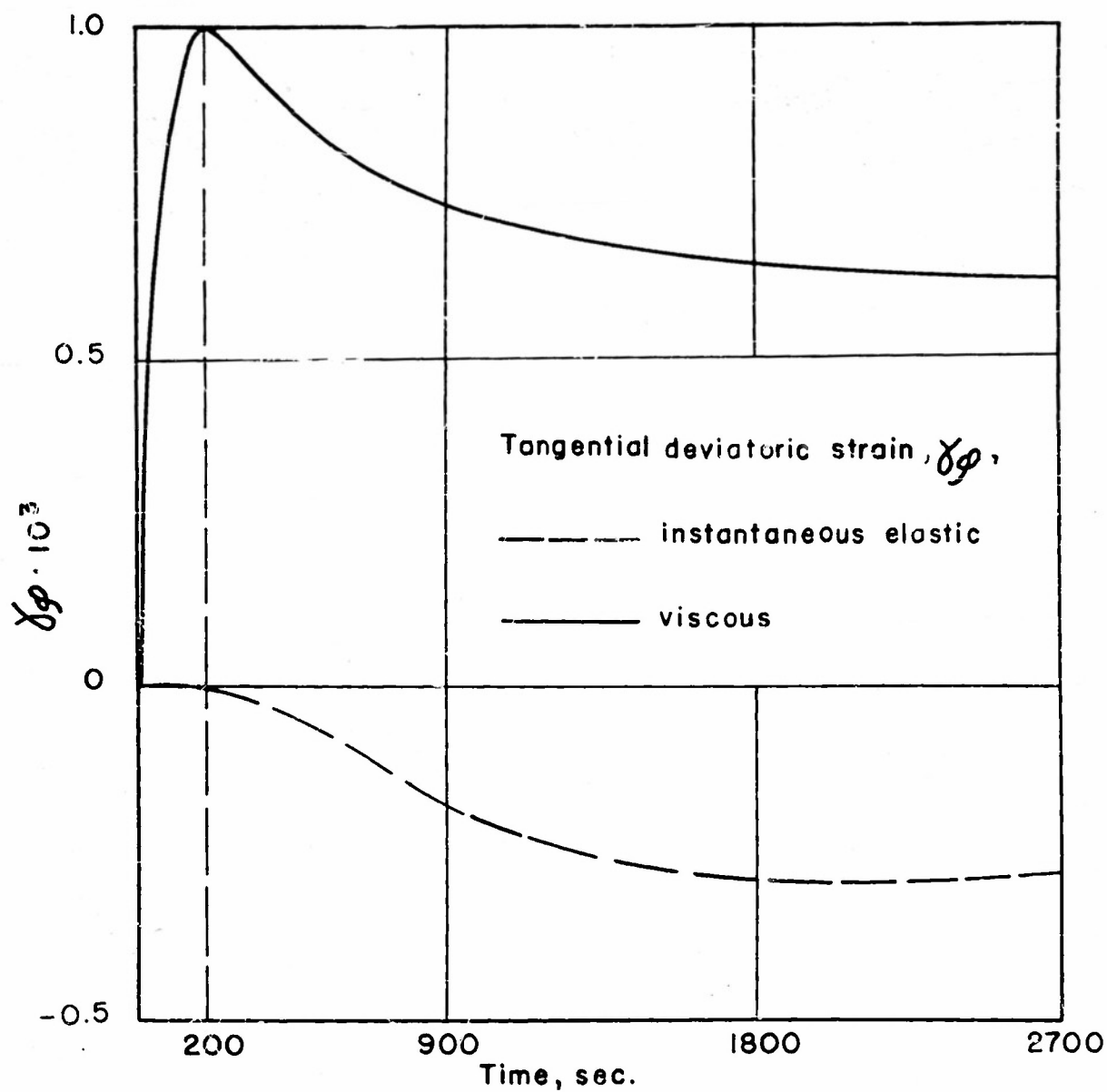
Fig. 5

The variation with time of the tangential deviatoric
instantaneous elastic and viscous strain at $r = .8b$
in sphere No. 4.
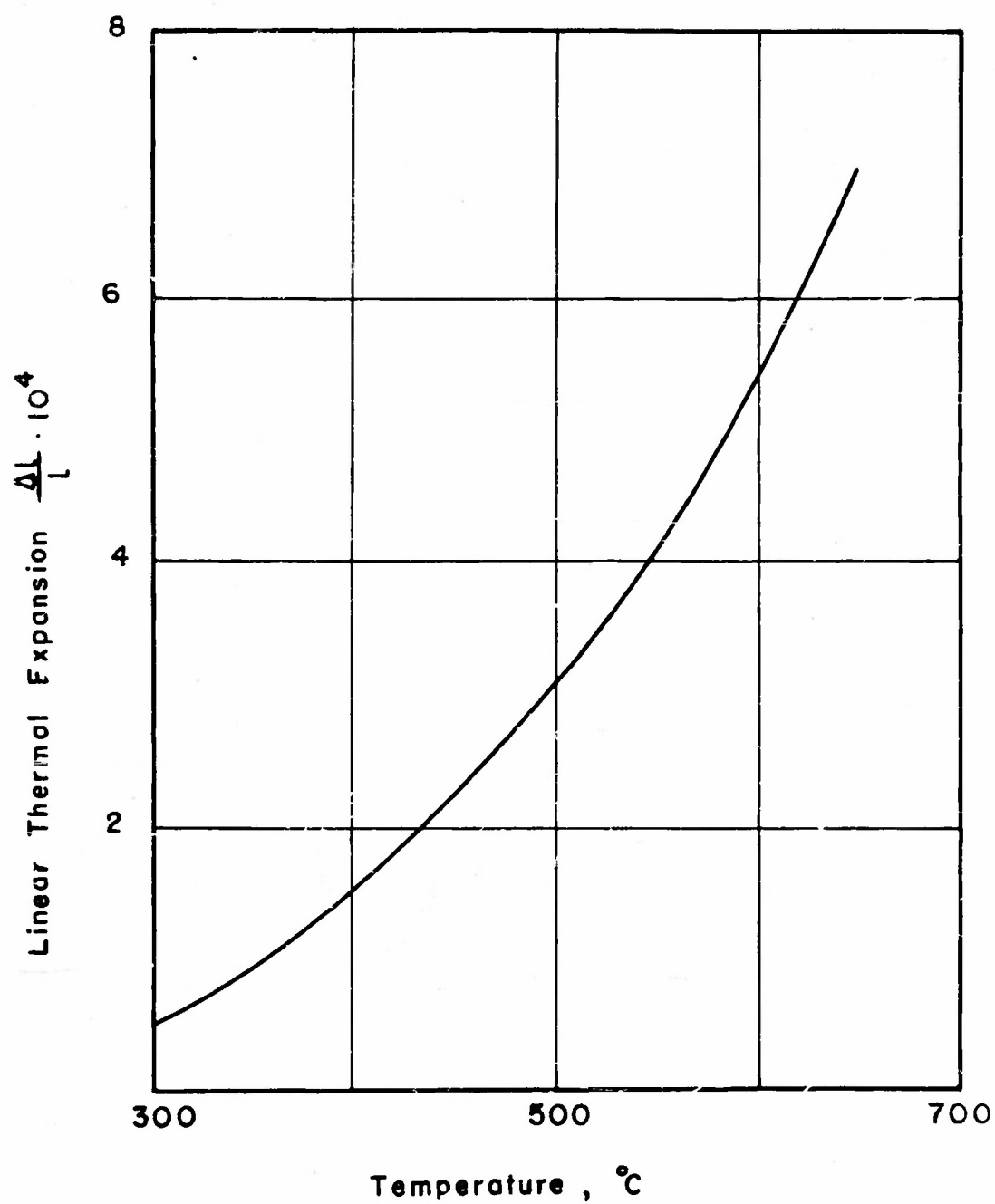
Fig. 6

The linear thermal expansion curve for
the glass used by Parsons.

Intermediate viscosity   **Low viscosity**

Fig. 7

A generalized Maxwell model exhibiting the important
viscoelastic phenomena in glass.

DISTRIBUTION LIST

for

Technical and Final Reports Issued Under
Office of Naval Research Project NR-064-388.   Contract Nonr-266(09)

Administrative, Reference and Liaison Activities of ONR

Chief of Naval Research
Department of the Navy
Washington 25, D.C.
  Attn: Code 438   (2)
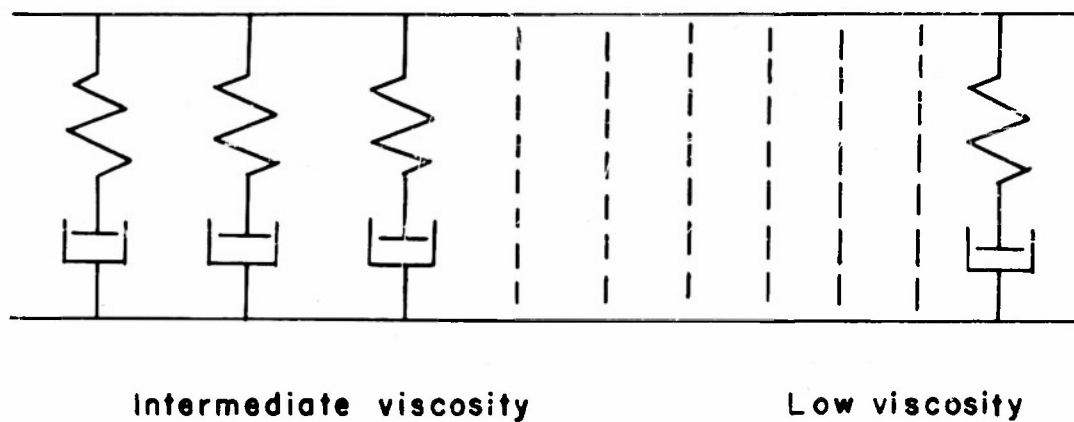   Code 416   (1)
         Code 421   (1)

Director, Naval Research Lab.
Washington 25, D.C.
  Attn: Tech. Info. Officer   (9)
         Technical Library   (1)
         Mechanics Division   (2)
         Code 3834 (J.P. Walsh)   (1)

Commanding Officer
Office of Naval Research
Branch Office
150 Causeway Street
Boston 10, Massachusetts   (1)

Commanding Officer
Office of Naval Research
Branch Office
346 Broadway
New York 13, New York   (1)

Commanding Officer
Officer of Naval Research
Branch Office
844 N. Rush Street
Chicago 11, Illinois   (1)

Commanding Officer
Officer of Naval Research
Branch Office
1000 Geary Street
San Francisco 24, California   (1)

Commanding Officer
Office of Naval Research
Branch Office
1030 Green Street
Pasadena, California   (1)

Contract Administrator, SE Area
Office of Naval Research
c/o George Washington University
707 22nd Street, N.W.
Washington 6, D.C.   (1)

Officer in Charge
Office of Naval Research
Branch Office, London
Navy No. 100
FPO, New York, N.Y.   (5)

Library of Congress
Washington 25, D.C.
  Attn: Navy Research Section   (2)

Department of Defense
Other Interested Government Activities

GENERAL

Research and Development Board
Department of Defense
Pentagon Building
Washington 25, D.C.
  Attn: Library (Code 3D-1075)   (1)

Armed Forces Special Weapons Project
P.O. Box 2610
Washington, D.C.
  Attn: Col. G. F. Blunda   (1)

ARMY

Chief of Staff
Department of the Army
Research and Development Division
Washington 25, D.C.
  Attn: Chief of Res. and Dev.   (1)

Office of the Chief of Engineers
Assistant Chief for Works
Department of the Army
Bldg. T-7, Gravelly Point
Washington 25, D.C.
  Attn: Structural Branch
      (R.L. Bloor)   (1)

Office of the Chief of Engineers
Asst. Chief for Military Construction
Department of the Army
Bldg. T-7, Gravelly Point
Washington 25, D.C.
  Attn: Structures Branch
      (H.F. Carey)   (1)

Engineering Research & Development Lab.
Fort Belvoir, Virginia
  Attn: Structures Branch   (1)

The Commanding General
Sandia Base, P.O. Box 5100
Albuquerque, New Mexico
  Attn: Col. Canterbury   (1)

Operations Research Officer
Department of the Army
Ft. Lesley J. McNair
Washington 25, D.C.
  Attn: Howard Brackney   (1)

Office of Chief of Ordnance
Research & Development Service
Department of the Army
The Pentagon
Washington 25, D.C.
  Attn: ORDTB   (2)

Commanding Officer
Ballistic Research Laboratory
Aberdeen Proving Ground
Aberdeen, Maryland
  Attn: Dr. C. W. Lampson   (1)

ARMY (cont.)

Commanding Officer
Watertown Arsenal
Watertown, Massachusetts
  Attn: Laboratory Division   (1)

Commanding Officer
Frankford Arsenal
Philadelphia, Pennsylvania
  Attn: Laboratory Division   (1)

Commanding Officer
Squier Signal Laboratory
Fort Monmouth, New Jersey
  Attn: Components and Materials
      Branch   (1)

NAVY
Chief of Bureau of Ships
Navy Department
Washington 25, D.C.
  Attn: Director of Research   (2)

Director
David Taylor Model Basin
Washington 7, D.C.
  Attn: Structural Mechanics Div. (2)

Director
Naval Engr. Experiment Station
Annapolis, Maryland   (1)

Director
Materials Laboratory
New York Naval Shipyard
Brooklyn 1, New York   (1)

Chief of Bureau of Ordnance
Navy Department
Washington 25, D.C.
  Attn: Ad-3, Technical Library   (1)

Superintendent
Naval Gun Factory
Washington 25, D.C.   (1)

Naval Ordnance Laboratory
White Oak, Maryland
RFD 1, Silver Spring, Maryland
  Attn: Mechanics Division   (2)

Naval Ordnance Test Station
Inyokern, California
  Attn: Scientific Officer   (1)

NAVY (cont.)

Commander, U.S. N.O.T.S.
Pasadena Annex
3202 E. Foothill Blvd.
Pasadena 8, California
  Attn: Code P5507   (1)

Commander, U.S. N.O.T.S.
China Lake, California
  Attn: Code 501   (1)

Chief of Bureau of Aeronautics
Navy Department
Washington 25, D.C.
  Attn: TD-41, Technical Library   (1)

Naval Air Experimental Station
Naval Air Materiel Center
Naval Base
Philadelphia 12, Pennsylvania
  Attn: Head, Aeronautical Materials
        Laboratory   (1)

Chief of Bureau of Yards & Docks
Navy Department
Washington 25, D.C.
  Attn: Code P-314   (1)

Officer in Charge
Naval Civil Engr. Research and Eval.
  Laboratory
Naval Station
Port Hueneme, California   (1)

Commander
U.S. Naval Proving Grounds
Dahlgren, Virginia   (1)

AIR FORCES
Commanding General
U.S. Air Forces
The Pentagon
Washington 25, D.C.
  Attn: Research & Development
        Division   (1)

Commanding General
Air Materiel Command
Wright-Patterson Air Force Base
Dayton, Ohio
  Attn: MCREX-B (E.H. Schwartz) (1)

AIR FORCES (cont.)

Office of Air Research
Wright-Patterson Air Force Base
Dayton, Ohio
  Attn: Chief, Applied Mechanics
        Group   (1)

OTHER GOVERNMENT AGENCIES
U.S. Atomic Energy Commission
Division of Research
Washington, D.C.   (1)

Argonne National Laboratory
P.O. Box 5207
Chicago 80, Illinois   (1)

Director
National Bureau of Standards
Washington, D.C.
  Attn: Dr. W. H. Ramberg   (1)

U.S. Coast Guard
1300 E Street, N.W.
Washington, D.C.
  Attn: Chief, Testing & Developing
        Division   (1)

Forest Products Laboratory
Madison, Wisconsin
  Attn: L. J. Markwardt   (1)

National Advisory Committee for
  Aeronautics
1724 F Street, N.W.
Washington, D.C.   (1)

National Advisory Committee for
  Aeronautics
Langley Field, Virginia
  Attn: Dr. E. Lundquist   (1)

National Advisory Committee for
  Aeronautics   (1)
Cleveland Municipal Airport
Cleveland, Ohio
  Attn: J. H. Collins, Jr. (1)

U.S. Maritime Commission
Technical Bureau
Washington, D.C.
  Attn: V. Russo   (1)

Contractors and Other Investigators
Actively Engaged in Related Research

Professor J. R. Andersen
Towne School of Engineering
University of Pennsylvania
Philadelphia 4, Pennsylvania   (1)

Professor M. Baron
Dept. of Civil Engineering and
  Engineering Mechanics
Columbia University
New York 27, New York   (1)

Dr. R. Bechmann
The Brush Laboratories Company
3714 Chester Avenue
Cleveland 14, Ohio   (1)

Professor L. Beedle
Fritz Engineering Laboratory
Lehigh University
Bethlehem, Pennsylvania   (1)

Professor C. B. Biezeno
Technische Hoogeschool
Nieuwe Laan 76
Delft, Holland   (1)

Dr. M. A. Biot
300 Central Park West
New York 24, New York   (1)

Professor R. L. Bisplinghoff
Dept. of Aeronautical Engineering
Massachusetts Institute of Technology
Cambridge 39, Massachusetts   (1)

Professor H. H. Bleich
Dept. of Civil Engineering and
  Engineering Mechanics
Columbia University
New York 27, New York   (1)

Professor J. A. Bogdanoff
Dept. of Civil Engineering
Purdue University
Lafayette, Indiana   (1)

Professor B. A. Boley
Dept. of Civil Engineering and
  Engineering Mechanics
Columbia University
New York 27, New York   (1)

Professor P. W. Bridgeman
Dept. of Physics
Harvard University
Cambridge 38, Massachusetts   (1)

Professor D. M. Burmister
Dept. of Civil Engineering and
  Engineering Mechanics
Columbia University
New York 27, New York   (1)

Dr. V. Cadambe
Assistant Director of the National
  Physical Laboratory of India
Hillside Road
New Delhi 12, India   (1)

Professor G. F. Carrier
Division of Applied Science
Pierce Hall
Harvard University
Cambridge 38, Massachusetts   (1)

Dr. D. Cheng
M. W. Kellogg Company
225 Broadway
New York, New York   (1)

Committee on Government Aided Research
Columbia University
313 Low Memorial Library
New York 27, New York   (2)

Mrs. H. Cooper
The Dell
Searingtown
Albertson, Long Island, New York (1)

Dr. Antoine E. I. Craya
Neyrpic
Boite Postale 52
Grenoble, France   (1)

Professor R. M. Davies
Department of Physics
University College of Wales
Aberystwyth, Wales
United Kingdom   (1)

Professor J. P. Den Hartog
Dept. of Mechanical Engineering
Massachusetts Institute of Technology
Cambridge 39, Massachusetts   (1)

Professor H. Deresiewicz
Dept. of Civil Engineering and
   Engineering Mechanics
Columbia University
632 West 125th Street
New York 27, New York   (1)

Dr. C. O. Dohrenwend
Rensselaer Polytechnic Institute
Troy, New York   (1)

Professor T. J. Dolan
Dept. of Theoretical and Applied
   Mechanics
University of Illinois
Urbana, Illinois   (1)

Professor L. H. Donnell
Dept. of Mechanics
Illinois Institute of Technology
Chicago 16, Illinois   (1)

Professor D. C. Drucker
Division of Engineering
Brown University
Providence 12, Rhode Island   (1)

Professor J. Duffy
Division of Engineering
Brown University
Providence 12, Rhode Island   (1)

Dr. W. Eckert
Watson Scientific Computing Laboratory
612 West 116th Street
New York 27, New York   (1)

Dr. H. Ekstein
Armour Research Foundation
Illinois Institute of Technology
Chicago 16, Illinois   (1)

Engineering and Industrial
   Experiment Station
University of Florida
Gainesville, Florida   (1)

Engineering Library
Columbia University
New York 27, New York   (1)

Professor E. L. Eriksen
University of Michigan
Ann Arbor, Michigan   (1)

Professor A.C. Eringen
Purdue University
Lafayette, Indiana   (1)

Dr. W. L. Esmeijer
Voorduinstraat 24
Haarlem, Holland   (1)

Professor E. A. Fox
Dept. of Mechanics
Rensselaer Polytechnic Institute
Troy, New York   (1)

Mr. M. Forray
1396 East 16th Street
Brooklyn 30, New York   (1)

Dr. F. Forscher
Westinghouse Atomic Power Division
P.O. Box 1468
Pittsburgh 30, Pennsylvania   (1)

Professor A. M. Freudenthal
Dept. of Civil Engineering and
   Engineering Mechanics
Columbia University
New York 27, New York   (1)

Professor B. Fried
Dept. of Mechanical Engineering
Washington State College
Pullman, Washington   (1)

Professor K. O. Friedrichs
New York University
Washington Square
New York, New York   (1)

Professor M. M. Frocht
Dept. of Mechanics
Illinois Institute of Technology
Chicago 16, Illinois   (1)

Professor J. M. Garrelts
Dept. of Civil Engineering and
   Engineering Mechanics
Columbia University
New York 27, New York   (1)

Professor J. A. Goff
University of Pennsylvania
Philadelphia, Pennsylvania   (1)

Dr. E. A. Gerber
Signal Corps Engineering Labs.
Fort Monmouth, New Jersey
  Watson Area   (1)

Mr. M. Goland
Midwest Research Institute
4049 Pennsylvania
Kansas City 2, Missouri   (1)

Professor J. N. Goodier
Division of Engineering Mechanics
Stanford University
Stanford, California   (1)

Professor L. E. Goodman
Dept. of Mechanics and Materials
University of Minnesota
Minneapolis 14, Minnesota   (1)

Professor R. J. Hansen
Massachusetts Institute of Technology
Cambridge 39, Massachusetts   (1)

Professor R. M. Hermes
College of Engineering
University of Santa Clara
Santa Clara, California   (1)

Professor G. Herrmann
Dept. of Civil Engineering and
  Engineering Mechanics
Columbia University
New York 27, New York   (1)

Professor M. Hetenyi
Northwestern University
Evanston, Illinois   (1)

Professor T. J. Higgins
Dept. of Electrical Engineering
University of Wisconsin
Madison 6, Wisconsin   (1)

Professor N. J. Hoff
Dept. of Aeronautical Engineering
  and Applied Mechanics
99 Livingston Street
Brooklyn 1, New York   (1)

Professor M. B. Hogan
Dept. of Mechanical Engineering
University of Utah
Salt Lake City 1, Utah   (1)

Professor D. L. Holl
Iowa State College
Ames, Iowa   (1)

Dr. J. H. Hollomon
General Electric Research Labs.
1 River Road
Schenectady, New York   (1)

Professor W. H. Hoppmann II
Dept. of Mechanical Engineering
The Johns Hopkins University
Baltimore 18, Maryland   (1)

Dr. G. Horvay
Knolls Atmoic Power Laboratory
General Electric Company
Schenectady, New York   (1)

Institut de Mathematiques
Universite
post. fah 55
Skoplje, Yugoslavia   (1)

Professor L. S. Jacobsen
Dept. of Mechanical Engineering
Stanford University
Stanford, California   (1)

Professor B. G. Johnston
Dept. of Civil Engineering
University of Michigan
Ann Arbor, Michigan   (1)

Dr. T. R. Kane
25-2 Valley Road
Drexel Hill, Pennsylvania   (1)

Professor K. Klotter
Division of Engineering Mechanics
Stanford University
Stanford, California   (1)

Professor W. J. Krefeld
Dept. of Civil Engineering and
  Engineering Mechanics
Columbia University
New York 27, New York   (1)

Professor B. J. Lazan
Dept. of Mechanics and Materials
University of Minnesota
Minneapolis 14, Minnesota   (1)

Professor E. H. Lee
Graduate Division of Applied
 Mathematics
Brown University
Providence 12, Rhode Island   (1)

Professor G. H. Lee
Rensselaer Polytechnic Institute
Troy, New York   (1)

Professor J. M. Lessells
Dept. of Mechanical Engineering
Massachusetts Institute of Technology
Cambridge 39, Massachusetts   (1)

Library, Engineering Foundation
29 West 39th Street
New York, New York   (1)

Professor P. Lieber
Rensselaer Polytechnic Institute
Troy, New York   (1)

Professor Hsu Lo
School of Aeronautics
Purdue University
Lafayette, Indiana   (1)

Professor C. T. G. Looney
Dept. of Civil Engineering
Yale University
New Haven, Connecticut   (1)

Dr. J. L. Lubkin
Midwest Research Institute
4049 Pennsylvania
Kansas City 2, Missouri   (1)

Professor J. F. Ludloff
School of Aeronautics
New York University
New York 53, New York   (1)

Professor J. N. Macduff
Department of Mechanical Engineering
Rensselaer Polytechnic Institute
Troy, New York   (1)

Dr. C. W. MacGregor
University of Pennsylvania
Philadelphia 4, Pennsylvania   (1)

Professor L. E. Malvern
Dept. of Applied Mechanics
Michigan State College
East Lansing, Michigan   (1)

Professor J. H. Marchant
Brown University
Providence 12, Rhode Island   (1)

Professor J. Marin
Dept. of Engineering Mechanics
Pennsylvania State University
State College, Pennsylvania   (1)

Dr. W. P. Mason
Bell Telephone Laboratories
Murray Hill, New Jersey   (1)

Dr. J. Miklowitz
U.S. Naval Ordnance Test Station
3202 E. Foothill Blvd.
Pasadena 8, California   (1)

Professor R. D. Mindlin
Dept. of Civil Engineering and
 Engineering Mechanics
Columbia University
632 West 125th Street
New York 27, New York   (15)

Dr. A. Nadai
136 Cherry Valley Road
Pittsburgh 21, Pennsylvania   (1)

Professor P. M. Naghdi
Dept. of Engineering Mechanics
University of Michigan
Ann Arbor, Michigan   (1)

Professor N. M. Newmark
207 Talbot Laboratory
University of Illinois
Urbana, Illinois   (1)

Professor J. Ormondroyd
Dept. of Engineering Mechanics
University of Michigan
Ann Arbor, Michigan   (1)

Professor W. R. Osgood
Dept. of Mechanics
Illinois Institute of Technology
Chicago 16, Illinois   (1)

Dr. G. B. Pegram
313 Low Memorial Library
Columbia University
New York 27, New York   (1)

Dr. R. P. Petersen
Director, Applied Physics Division
Sandia Laboratory
Albuquerque, New Mexico (1)

Mr. R. E. Peterson
Westinghouse Research Laboratories
East Pittsburgh, Pennsylvania (1)

Professor A. Phillips
Dept. of Mechanical Engineering
Stanford University
Stanford, California (1)

Professor C. Pickett
Dept. of Mechanics
University of Wisconsin
Madison 6, Wisconsin (1)

Dr. H. Poritsky
General Engineering Laboratory
General Electric Company
Schenectady, New York (1)

Professor W. Prager
Graduate Division of Applied
  Mathematics
Brown University
Providence 12, Rhode Island (1)

Dr. F. Press
Lamont Geological Observatory
Torrey Cliff
Palisades, New York (1)

RAND Corporation
1700 Main Street
Santa Monica, California
   Attn: Dr. E. H. Plesset (1)

Dr. S. Raynor
Armour Research Foundation
Illinois Institute of Technology
Chicago 16, Illinois (1)

Professor E. Reissner
Dept. of Mathematics
Massachusetts Institute of Technology
Cambridge 39, Massachusetts (1)

Professor H. Reissner
Dept. of Aeronautical Engineering
  and Applied Mechanics
Polytechnic Institute of Brooklyn
99 Livingston Street
Brooklyn 1, New York (1)

Dr. K. Robinson
800 Cranford Avenue
Bronx 70, New York (1)

Professor L. Rongved
Dept. of Engineering Mechanics
Pennsylvania State University
State College, Pennsylvania (1)

Professor M.A. Sadowsky
Dept. of Mechanics
Rensselaer Polytechnic Institute
Troy, New York (1)

Professor M. G. Salvadori
Dept. of Civil Engineering and
  Engineering Mechanics
Columbia University
New York 27, New York (1)

Mr. A. Schacknow
20-35 Seagirt Boulevard
Far Rockaway, New York (1)

Dr. F. S. Shaw
Superintendent
Structures & Materials Division
Aeronautical Research Laboratories
Box 4331, G.P.O. Melbourne
Victoria, Australia (1)

Dr. D. T. Sigley
American Machine and Foundry Company
511 Fifth Avenue
New York, New York (1)

Professor C. B. Smith
Department of Mathematics
Walker Hall
University of Florida
Gainesville, Florida (1)

Professor C. R. Soderberg
Dept. of Mechanical Engineering
Massachusetts Institute of Technology
Cambridge 39, Massachusetts (1)

Sir Richard V. Southwell
The Old House
Trumpington
Cambridge, England (1)

Professor E. Sternberg
Illinois Institute of Technology
Chicago 16, Illinois   (1)

Professor J. J. Stoker
New York University
Washington Square
New York, New York   (1)

Mr. R. A. Sykes
Bell Telephone Laboratories
Murray Hill, New Jersey   (1)

Professor P. S. Symonds
Graduate Division of Applied
  Mathematics
Brown University
Providence 12, Rhode Island   (1)

Professor J. L. Synge
Dublin Institute for Advanced Studies
School of Theoretical Physics
64-65 Merrion Square
Dublin, Ireland   (1)

Professor F. K. Teichmann
Dept. of Aeronautics
New York University
Bronx 53, New York   (1)

Professor S. P. Timoshenko
School of Engineering
Stanford University
Stanford, California   (1)

Professor C. A. Truesdell
Graduate Institute for Applied
  Mathematics
Indiana University
Bloomington, Indiana   (1)

Professor K. S. Van Dyke
Department of Physics
Scott Laboratory
Wesleyan University
Middletown, Connecticut   (1)

Dr. I. Vigness
Naval Research Laboratory
Anacostia Station
Washington, D.C.   (1)

Dr. Leonardo Villena
Av. de La Habana. 147
Madrid, Spain   (1)

Professor E. Volterra
Dept. of Mechanics
Rensselaer Polytechnic Institute
Troy, New York   (1)

Mr. A. M. Wahl
Westinghouse Research Laboratories
East Pittsburgh, Pennsylvania   (1)

Professor C. T. Wang
Dept. of Aeronautics
New York University
University Heights
Bronx 53, New York   (1)

Dr. R. L. Wegel
RFD 2
Peekskill, New York   (1)

Professor E. E. Weibel
Dept. of Mechanical Engineering
University of Colorado
Boulder, Colorado   (1)

Professor J. Weiner
Dept. of Civil Engineering and
  Engineering Mechanics
Columbia University
New York 27, New York   (1)

Professor A. Weinstein
Institute for Fluid Dynamics and
  Applied Mathematics
University of Maryland
College Park, Maryland   (1)

Professor D. Young
Yale University
Winchester Hall
15 Prospect Street
New Haven 11, Connecticut   (1)

Armed Services Technical Information Agency

AD 37716

Reproduced by

DOCUMENT SERVICE CENTER
KNOTT BUILDING, DAYTON, 2, OHIO

UNCLASSIFIED